ORIGINAL ARTICLE VW Applied Sciences

DOI: 10.36297/vw.applsci.v2i1.36 ISSN: 2582-5615

VW Applied Sciences, Volume: 2, Issue: 1, 64-73

Mathematical Modeling of the Land Model on Human Myocyte

Fisal Asiri[1]

[1]Department of Mathematics, College of Science, Taibah University, Medina, Saudi Arabia
Author Email: fasiri@taibahu.edu.sa

Research publication from M.S. Thesis, submitted at School of Mathematics and Statistics, University of Glasgow, United Kingdom

Received: Jan. 09, 2020
Accepted: March 29, 2020
Published online: April 01, 2020

Abstract: The Land model encompasses modelling of the contraction of the cardiac muscle, based on the evaluation of the development of tension in cardiomyocytes in human heart muscle. The paper presents the mathematical modeling of myocyte by using the Land model, which was developed based on real experimentation. The mathematical models simulated in this project were based on the existing models in the Land model. The Land model aimed to strike a balance between modelling detail and the ability to parameterize the model using available data. We simulated different parameters presented in the Land model to establish the behavior of the tension developed in the cardiac myocytes of the human heart. The model was verified with extensive experimental data on the effects of various parameters such as calcium, T_{ref} on the tension developed in the myocyte cells at physiological room temperature. Several models for cardiac myocyte contraction have been developed to date, although earlier models did not include sarcomere shortening during twitch. They were primarily focused on simplification of the description of crossbridge kinetics, their dependence on Ca2+ dynamics, and careful reproduction of the existing experimental data on steady-state and dynamic force-calcium relationships.

Keywords: Mathematical modeling, Cardiac cell, Land model, Human myocyte,

1. Introduction

The Land model encompasses modelling of the contraction of the cardiac muscle, based on the evaluation of the development of tension in cardiomyocytes in human heart muscle; it was developed by Land et al [1] using experimental data. The Land model entails tropomyosin kinetics, troponin C kinetics, the cellular viscoelastic response and a three-state cross-bridge model which accounts for the distortion of cross-bridges. It was parameterized using diff t experimental data obtained in human cardiomyocytes at the physiological body temperature, including the passive and viscoelastic properties of isolated myocytes, the steady-state force calcium relationship at diff t sarcomere lengths along with changes in tension following a rapid increase or decrease in length, after constant velocity shortening, and dynamic changes in tension generation during length perturbations in isolated myocytes.[2-8]

There was a lack of experimental data from human cardiac myocytes at the physiological body temperature for quantitative understanding of clinically relevant cardiac function and development of whole-organ computational models. Specifically, important measurements to characterize changes in tension development in human cardiomyocytes that occur with perturbations in cell length were not available. To address this deficiency, they presented an experimental data set collected from skinned human cardiac myocytes. This data set used in the Land model is the fi characterization of length and velocity-dependence of tension generation in human skinned cardiac myocytes at body temperature. [9-17]

In this work, we will use the Land model to study the human myocyte contraction in detail, and in particular how different parameters affect myocyte contraction behaviors. First, we introduce the passive viscoelastic model, then active tension model which includes thin Filament kinetics, the cross-bridges model and active tension model. We will then examine the Land model and the relevant parameters that Land et al used to establish the behavior of the cardiac muscle.

2. Passive Viscoelastic Model

The passive viscoelastic model of the human cardiac myocytes was developed by analyzing the unique viscous response of the myocytes. This unique viscous response results from the molecule titin, which is part of the contractile apparatus of the cardiac muscle. It is assumed that the passive response is independent of other experimental data on active tension presented in this model.

In Land's experiments [13], the viscous component represented 44±5% of total passive force, and 75% of this force decayed within 92±24 ms. On shortening, the

viscous response is significantly lower, potentially due to a much faster decay rate and recovery during the duration of the shortening step. The passive response was modelled using a three- parameter model similar to a standard linear solid, consisting of a dashpot and spring in series, in parallel with another spring, as shown in Fig. 1. This model was chosen for its simplicity and its ability to capture the passive and viscoelastic response. To reproduce the typical exponential force-length relationship seen in previous experiments in isolated cells and cardiac tissue, the parallel spring.

$F_1 = a(e^{bc} - 1)$

has an exponential stress-strain relationship and:

$F_2 = akC_s,$

is a linear spring.

The active contractile element TA is introduced in later sections and has zero stiffness when the myocyte is not in an active contraction state. The dashpot element Fd (see fi 4.1) has separate parameters for shortening and lengthening to accommodate the diff in viscous forces observed.

$$F_d = \begin{cases} a\eta_l \frac{dC_d}{dt}, & \frac{dC_d}{dt} > 0, \\ a\eta_s \frac{dC_d}{dt}, & \frac{dC_d}{dt} < 0. \end{cases}$$

This can be understood in analogy to electrical circuitry. Two elements in series have the same forces, which are F2 = Fd in our case (passive viscoelastic model), and the total strain (C) is the sum of two strains which are:

C = Cs + Cd,

where Cd is the strain of dashpot and Cs is the strain of spring. This yield;

$$\begin{aligned} F_{total}(c) &= F_1 + F_2, \\ &= a(e^{bc} - 1) + aKC_s. \end{aligned}$$

This represents the total force of the viscoelastic element (titin) as a function of the strain

(C) (or extension ratio, λ = SL/SL0.) C and λ are related through SL

$$C = \lambda - 1 = \frac{SL}{SL_0} - 1.$$

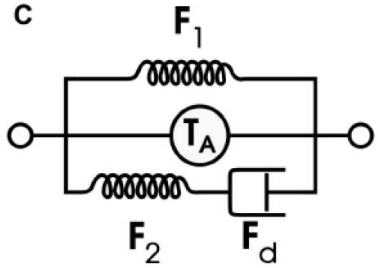

Figure 1: Schematic illustration of the myocyte model. F1 is the parallel elastic element, F2 is the series elastic element, Fd is the viscous dashpot element, and TA is the active contractile element, cited from [13].

Furthermore,

$$F_{\text{total}}(c) = F_1 + F_d,$$

$$= a(e^{bc} - 1) + \begin{cases} a\eta_l \frac{dC_d}{dt}, & \frac{dC_d}{dt} > 0, \\ a\eta_s \frac{dC_d}{dt}, & \frac{dC_d}{dt} < 0, \end{cases}$$

where s is for shortening and l for lengthening.

3. The Active Tension Model

The force generating apparatus of the cell consists primarily of two types of fi ts, thick fi ts and thin fi ents. Thin filaments are composed of actin, tropomyosin, and troponins, including troponin C and troponin I. Thick fi ments are made up of myosin cross-bridges. Active tension is generated by myosin cross-bridges attaching to binding sites on actin on the thin fi t, and then performing a power stroke. cross- bridges consist of a head region, which rotates during a power stroke, and a tail region (the neck region of the myosin molecule) which is distorted. The restoring forces on the spring-like tail are responsible for force generation. As the fi ts slide past each other, the distortion of the cross-bridges tail ,which is generated by the power stroke is reduced, generating less force. By detaching, returning to their resting length, and re-attaching to a new binding site and once again performing a power stroke, cross-bridges restore their maximal force generating ability.

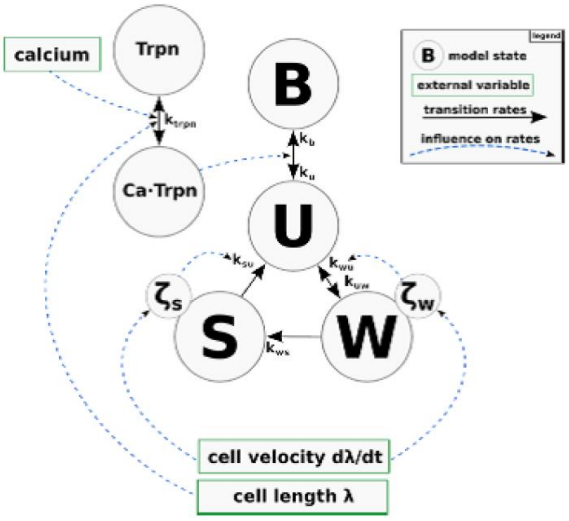

Figure 2: Cross-bridge dynamics during active contraction, cited from [13].

4. Thin Filament Kinetics

Figure 4.2 describes the cross-bridge dynamics during active contraction, in which B represents the blocked state, which means Troponin and Tropomyosin cover the active site on actin (i.e., myosin head cannot bind to the active site on actin). In the resting state,

tropomyosin, which winds helically around actin on the thin fi t, satirically blocks the binding sites for myosin on actin. It is held in this 'blocking' position by troponin I, another thin fi ment protein. When the cell is electrically activated, the calcium concentration rises. Calcium ions Ca2+ from the cytosol bind to the regulatory binding site on troponin C. This causes troponin C to open a binding pocket for troponin I, causing troponin I to preferentially move away from holding tropomyosin in the 'blocked' position U, with U is an unbinding state which means the active sites on actin are uncovered, allowing cross-bridges to bind (i.e., myosin head -binds to the active site on actin and forms a cross-bridges, W). W is the pre power stroke state which means the myosin head moves at the hinge region (powers stroke state) causing the actin to slide past the myosin. ATP binds to the myosin head causing the myosin head to release the actin, with everything going back to the initial state (post power stroke stage, S) and generating tension. Furthermore, ζw and ζs are the mean distortions of the cross bridges in the weak and strong states respectively.

The kinetics of filaments are described by the interaction between various elements such as calcium ions, troponin C, troponin I and tropomyosin to regulate availability of myosin binding sites on actin. Activation of the thin filaments shows highly cooperative behavior, with small changes in intracellular calcium leading to potentially high changes in force. The main biophysical reason for this behavior relates to the end-to-end overlap of tropomyosin molecules. A simple and phenomenological representation of cooperative activation is chosen, as it is better suited for applications in multiscale modelling. The dynamics of calcium ions binding is

$$\frac{\mathrm{dCaTRPN}}{\mathrm{dt}} = \mathrm{k_{TRPN}}\left(\frac{[\mathrm{Ca}^{2+}]_i}{[\mathrm{Ca}^{2+}]_{\mathrm{T50}}}\right)^{\mathrm{n_{TRPN}}}(1-\mathrm{CaTRPN}) - \mathrm{CaTRPN},$$

in which [Ca^{2+}]i is the intracellular calcium concentration. [Ca^{2+}]T50 is the concentration of calcium required to bind 50% of troponin. Equation 4.2.1 can be solved analytically, with the following method: For simplicity we write CaT instead of CaTRPN. We assume [Ca^{2+}]i is a constant and independent of time, then we can state;

$$\left(\frac{[\mathrm{Ca}^{2+}]_i}{[\mathrm{Ca}^{2+}]_{\mathrm{T50}}}\right)^2 = a.$$

So

$$\frac{\mathrm{dCaT}}{0.1(a(1-\mathrm{CaT})-\mathrm{CaT})} = \mathrm{dt},$$

$$\frac{\mathrm{dCaT}}{(a-\mathrm{aCaT\text{-}CaT})} = 0.1\mathrm{dt},$$

$$\frac{\log(a-(1+a)CaT)}{-(1+a)} = 0.1\mathrm{t}+\mathrm{C},$$

$$\log(a-(1+a)CaT) = -(1+a)0.1\mathrm{t}+\mathrm{C},$$

$$a-(1+a)CaT = e^{(-(1+a)0.1\mathrm{t}+\mathrm{C})},$$

$$\mathrm{CaT(t)} = \frac{\mathrm{a\text{-}Ne}^{-(1+a)0.1\mathrm{t}}}{1+a},$$

with N being a constant.

Using the initial condition t =0 then:

$$N = a-(1+a)CaT_0.$$

$$\text{If } [\mathrm{Ca}^{2+}]_i \le [\mathrm{Ca}^{2+}]_{\mathrm{T50}} \Rightarrow 0 \le a \le 1, \text{ where}$$

$$a = \left(\frac{[\mathrm{Ca}^{2+}]_i}{[\mathrm{Ca}^{2+}]_{\mathrm{T50}}}\right)^2,$$

• If [Ca^{2+}]i > [Ca^{2+}]T50 then a > 1 and still 0 < N < a, so the corresponding time course of CaTRPN is shown in Fig. 4.

CaTRPN represents the fraction of troponin C units with calcium bound to its reg- ulatory binding site. The parameter kTRPN = 0.1/ms represents the unbinding rate, nTRPN = 2, which is the cooperativity of the calcium-troponin C binding rate. The parameter [Ca2+]T 50, which describes the half-activation point, is not consistent between species. The troponin concentration CaTRPN drives the unblocking of tropomyosin, as represented by the fraction of blocked myosin binding sites on actin, denoted by B:

$$\frac{dB}{dt} = k_b.\mathrm{CaTRPN}^{\frac{nTm}{2}}.U - K_u.\mathrm{CaTRPN}^{\frac{nTm}{2}}.B,$$

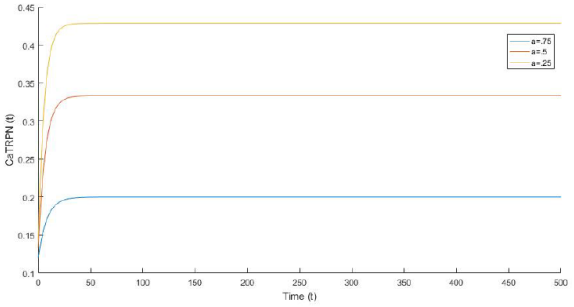

Figure 3: Diagram of CaTRPN for an arbitrary choice of parameters, when 0 < a < 1.

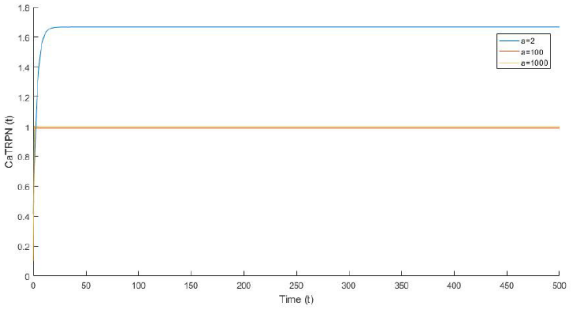

Figure 4: Diagram of CaTRPN for an arbitrary choice of parameters, when a > 1.

where kb and ku represent the transition rates for B and U states respectively. Equation.4.2.11 is not simple

to solve analytically because it depends on the two variables U and B.

The states included the fi 4.2 entail the blocked state B, the unbound cross-bridges state U, the pre-power stroke state W and the force generating state S. Both the states 'W' and 'S' in the fi have an additional state, keeping track of the mean distortion of cross-bridges in this state. Calcium binding to troponin C drives the transition between states 'B' and 'U'.

5. The Cross-bridges Model

The cross-bridges model for the generation of force was developed using a three-state cycle of the cross-bridges with unbound (U), pre-power stroke (W) and post-power stroke (S) states, as well as a model of the distortion decay that traces the average distortion of the cross-bridges in the pre-power stroke (W) and post-power stroke (S) states, as shown in Fig. 2:

$$U = (1 - B) - S - W.$$

Above equation is obtained from the conversion of different states shown in Fig. 2.

$$\frac{dW}{dt} = k_{uw}U - k_{wu}W - k_{ws}W - \gamma_{wu}W,$$
$$\frac{dS}{dt} = k_{ws}W - k_{su}S - \gamma_{su}S.$$

The parameters γ_{su} and γ_{wu} represent the cross-bridges unbinding rates in the pre-power stroke (W) and post-power stroke (S) states provided by a model of distortion decay. The distortion decay model is given by:

$$\frac{d\eta_w}{dt} = A_w\frac{d\lambda}{dt} - c_w\eta_w,$$
$$\frac{d\eta_s}{dt} = A_s\frac{d\lambda}{dt} - c_s\eta_s,$$
$$\gamma_{wu} = \gamma_w|\eta_w|,$$
$$\gamma_{su} = \begin{cases} \gamma_s(-\eta_s - 1), & \eta_s + 1 < 0, \\ \gamma_s\eta_s, & \eta_s + 1 > 1, \\ 0, & \text{if } \eta_s + 1 \epsilon [0, 1] \text{ or otherwise,} \end{cases}$$

in which, Aw and As relate to the magnitude of the instantaneous response to distortion and c_w and c_s relate to the decay rate of distortion. All variables with the subscript 'w' relate to the pre-powerstroke state W, and variables with the subscript 's' relate to the post-powerstroke state S. The variable λ indicates the cell length relative to the resting length, in Land's model. It is further assumed that the cross-bridges bind with no dis- tortion in the pre-powerstroke state. In addition, the cross-bridges do not maintain the distortion when transitioning from W to S states with ηs = 0, indicating the absence of additional distortion to that particular power stroke.

In the absence of changes in the length of the cells, ηw = ηs = 0. The total tension during active contraction is given by: Ta= number of crossbridges ∗ cross-bridges stiffness ∗ powerstroke ∗ distortion ∗ S. When distortion in both powerstrokes is considered, the total tension is given by:

Ta = (ζs + 1)S + ηw W.

In a cycle of reactions, such as in our cross-bridges model, it is typically easier to parameterize based on the steady-state occupation of states and an overall rate of cycling, which govern both forward and backward rates. The steady-state occupation can be more easily constrained using a prior or fi value, as it is less species-dependent, while the overall rate of cycling governs the kinetics of tension development and is likely to vary significantly between species. Thus, the following defined are introduced:

- rs - steady-state duty ratio S/(U+W+S)
- rw - the steady-state ratio between pre-powerstroke and non-strongly bound = steady-state W/(U+W)

TRPN50 = value of CaTRPN, where B=0.5 in steady state.

The above defined values help to parameterize the model, because it is easier to provide a good initial estimate for rs, rw and TRPN50. Assuming that rs=0.25, TRPN50 = 0.35 and rw = 0.5, then the derived parameters used in the model equations are given by:

$$k_{wu} = k_{uw}(1/r_w - 1) - k_{ws},$$
$$k_{su} = k_{ws}r_w(1/r_s - 1),$$
$$k_b = k_u\text{CaTRPN}^{nTm}/(1 - r_s - (1 - r_s)r_w).$$

In equation 4.2.16, the magnitude of instantaneous distortion in the W and S states is assumed to be equal because they reflect the distortion induced by relative movement of the filaments,

$$A_s = A_w = A_{eff}r_s/((1 - r_s)r_w + r_s).$$

Assuming the distortion decay rates to be proportional to steady-state cross-bridges cy- cling rates:

$$c_w = \phi k_{uw}U/W = \phi k_{uw}((1 - r_s)(1 - r_w))/((1 - r_s)r_w),$$
$$c_s = \phi k_{ws}W/S = \phi k_{ws}((1 - r_s)r_w/r_s).$$

Basically, there are four states that include Blocked, Unbound, Weak and Strong. These are all possible states of the cross-bridge. The Weak and Strong states diff from the other states in that have a mean distortion associated to them, ζw and ζs. Therefore, this model explains the changes of the four states, as well as the changes of the mean distortion.

6. The Length-Dependence of Tension

Another key aspect of tension generation in the heart is the increase in generated force with an increase in myocyte length. At the organ level, this phenomenon gives rise to the 'Frank-Starling' effect [13], where an increase in end-diastolic volume leads to an increase in the volume of blood ejected, ensuring a balance of fl w in and out of the heart. The molecular mechanisms underlying these effects have not been fully resolved. Land et al [13] assumed that the phenomenological

model represented the cellular effects that are defined by a shift in the intracellular calcium sensitivity and an increase in the maximum tension that is produced with length, as shown below:

$$[Ca^{2+}]_{T50} = [Ca^{2+}]^{ref}_{T50} + \beta_1(\min(\lambda, 1.2) - 1),$$
$$h(\lambda) = \max(0, h'(\min(\lambda, 1.2)),$$
$$h'(\lambda) = 1 + \beta_0(\lambda + \min(\lambda, 0.87) - 1.87),$$

in which, the parameter β0 represents the change in maximal tension; based on changes in fi t overlap, and β1 captures the change in calcium sensitivity. Therefore, the total active tension of the complete model is given by:

$$T_a = h(\lambda)\frac{T_{ref}}{r_s}((\xi_s + 1)S + \xi_w W),$$

where T_{ref} is the maximal active tension at resting length.

Length dependency encompasses the interactions between the length and calcium and cross-bridges dynamics during the contraction process. The process of crossbridge activation tends to increase with an increase in the length of the sarcomere during the contraction process in the cardiomyocytes. Theoretically, the increase in the cross-bridges activation due to increased length could result from the increase in the number of cross- bridges attached or cross-bridges strain. In addition, the number of cross-bridges tends to increase with an increase in the rate of cross-bridges attachment. In this case, a lower cross-bridges detachment rate or an increase in the calcium concentration in the sarcoplasm could also contribute an increase in the activation of the cross-bridges. The concentration of calcium is however independent of the length of the sarcomeres [3].

Changing the length of the sarcomeres has effects on the rate of attachment and de- tachment of cross-bridges to the activated and exposed binding sites on the actin. As a muscle fi er does not gain or lose volume as it changes length, the fi er must have a larger diameter when it is at a shorter length [21]. The hexagonally packed lattice of myofilaments in each sarcomere will then be more widely spaced, changing the distance between the myosin heads and the thin fi ts where they must bind to form cross- bridges [18]. The heads are located on the ends of hinged arms containing myosin light chains, which are canted away from the longitudinal axis of the thick fi ment. When the sarcomere is at a long length, the myosin heads barely fi between the thick and thin fi ts, so they are close and can bind rapidly to form cross-bridges.

The short distance between the myosin heads and actin binding sites also increases the strength of the actomyosin bond, which would reduce the probability of cross-bridges detachment. At short lengths, the myosin heads are less favorably disposed, and their binding may also be affected adversely by the double-overlap of the thin fi ts [2]. These effects are particularly significant at lower levels of activation, where activated binding sites are scarcer on the thin filaments [13]. The total result is indicated in Fig. 5, which is based on models and data from existing literature.

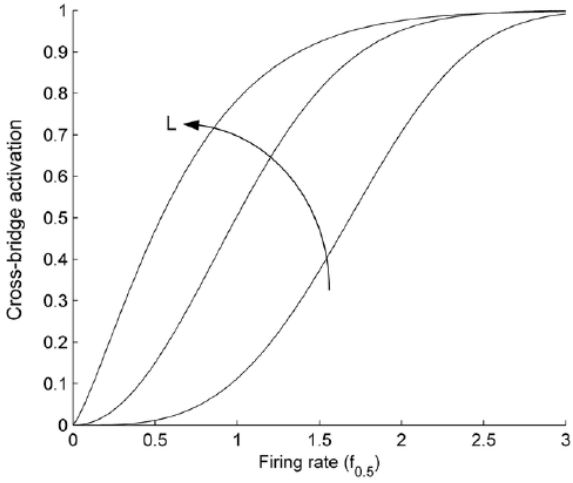

Figure 5: Length Dependence of Cross-bridge Activation, cited from [2].

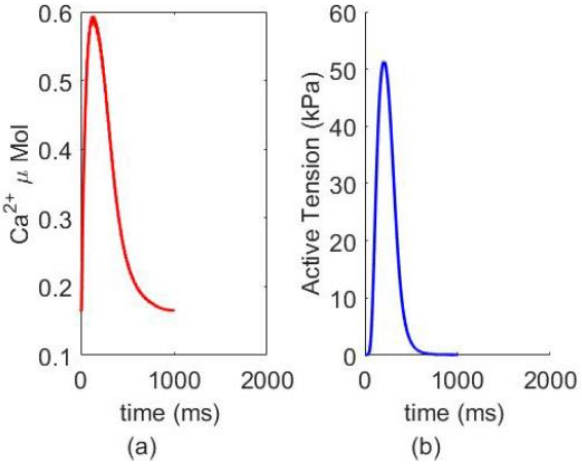

Figure 6: Isometric contraction with stretch ratio λ = 1.0, using prescribed intracellular calcium transients.

The activation of the cross-bridges is measured as a percentage of the maximum tension generation for a specific amount of overlap of the myofilament. The change in sarcomere length also infl the kinetics of calcium which control activation and con- traction in the cardiac muscle. The cisterns from which the calcium is released appear to be tethered to the Z-plates at a location near the middle of the actin-myosin overlap when the muscle is at optimal length. Calcium tends to diff over long distances at longer lengths to reach the actin binding sites [21]. In this case, the rise periods of the contraction are longer in calcium activation [13]. In addition, the rate of cross-bridges attachment increases while the rate of detachment decreases proportionally with the length of the sarcomere.

7. Results

The Myocyte model is implemented in MATLAB and solved using an ode15 solver with adaptive time

stepping. An, ode-15 solver was chosen because the mathematical model is stiff. A problem is said to be stiff if the solution being sought varies slowly, but there are nearby solutions that vary rapidly, so the numerical method must take small steps to obtain satisfactory results. This model demonstrates stiffness. The syntax for ode-15 is, [t,y] = ode15s(odefun,tspan,y0), where tspan = [t0tf].The solver integrates the system of diff tial equations y=f(t,y) from t0 to tf with initial conditions y0. Each row in the solution array y corresponds to a value returned in column vector t. MATLAB code was provided by Dr. Hao Gao, and is adopted from [13].

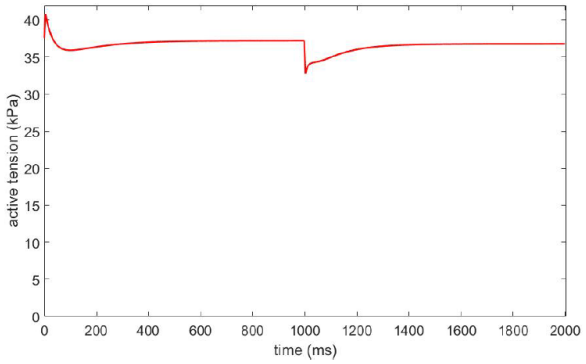

Figure 7: Effects of the calcium parameter on the tension in the cardio myocytes for an isotonic experiment.

We examine the isometric contraction with stretch ratio λ = 1.0, using prescribed intracellular calcium transients shown in Fig. 6(a). Fig. 6(b) is the corresponding developed tension. Active tension increases with increased Ca2+, and reaches the peak tension (50kPa) at 220ms, while Ca2+ reaches peak at 120ms, which is earlier than the peak tension. After reaching the peak, Ta decreases with decreased intracellular Ca2+.

Secondly, we model the release experiment, in which the intracellular Ca2+ is maintained with a constant level (30μMol), and the myocyte is stretched to 1.005 within 10ms, then held with fi length at a stretch ratio until 1000ms, and then allowed to contract with a constant contraction velocity within 5ms to return to its rest length, or λ = 1.0. Finally, the myocyte is held at a constant stretch ratio of 1.0 until 2000ms. Figure 4.7 shows the time course of active tension during all of the release experiments. From fi 4.7, we can see that the active tension increases quickly in the beginning because of the change in stretch ratio from 1 to 1.005 in 10ms, and that later it decreases since the stretch is fixed at a constant value, gradually reaching a steady state with an active tension of 37kPa. From 1000ms to 1005 ms, the myocyte shortens to its rest length, because the active tension is velocity dependent. Thus, it decreases with a minimum value of 33kPa. After 1005ms, since the stretch ratio is fi again, the active tension recovers to a higher level and reaches a steady state after 1500ms, with the final active tension being around 36.5kPa.

We examine the isometric contraction of the cardiac muscle at different stretch ratios: 0.90, 1.00, 1.10 and 1.20, using the intracellular calcium transients described in fi 4.8(a). Figure 4.8(b) shows the corresponding active tensions developed at the diff t stretch ratios. Active tension developed in the muscle increases steadily as Ca2+ transient increases up to the peak tensions of 10kPa, 50kPa, 120kPa and 170kPa at different stretch ratios: 0.90, 1.00, 1.10 and 1.20 respectively. However, the Ca2+ transient reaches peak at 0.6μM , which is higher than the amount required for achieving the highest peak tension at 1.2 stretch ratios of 0.55μM Ca2+ transient.

We then examine the isometric behavior of the tension developed in the muscle due to variation of the intracellular calcium profit at different stretch ratios. The intracellular Ca2+ varies with diff t values of the stretch. In this case, we were able to establish the effects of stretch ratios and Ca2+ on the tension developed in the muscle as shown in fi4.9. The tension developed at the stretch ratio of 0.9 is 20kPa, while the tension developed at 1.0 stretch ratios is 30kPa. In addition, the tension developed at stretch ratio of 1.1 and 1.2 are 40kPa and 50kPa respectively. It is observed in fi 4.9 that a higher stretch ratio contributes to the development of high active tension in the muscle. Moreover, the active tension increases steadily, initially with increased intracellular calcium at diff t stretch ratios up to specific peak values.

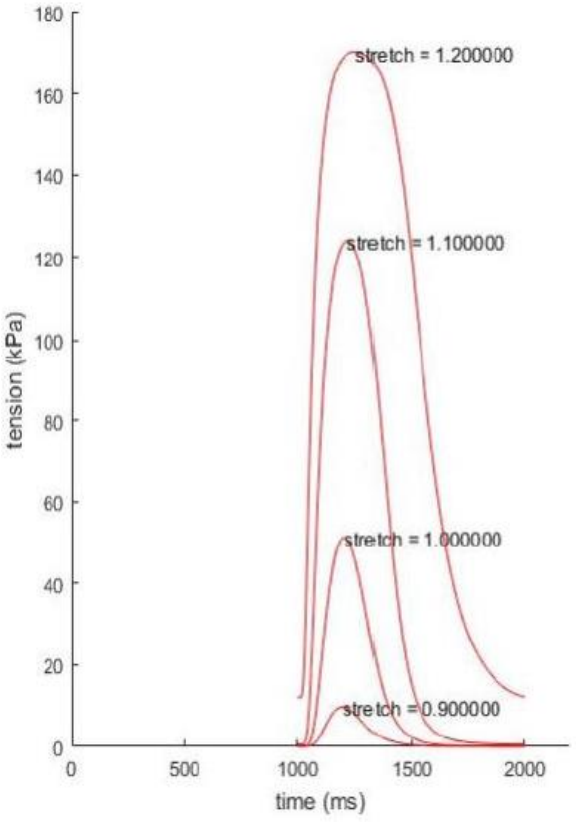

Figure 8: Isometric contraction of the cardiac muscle at different stretch ratios: 0.90, 1.00, 1.10 and 1.20.

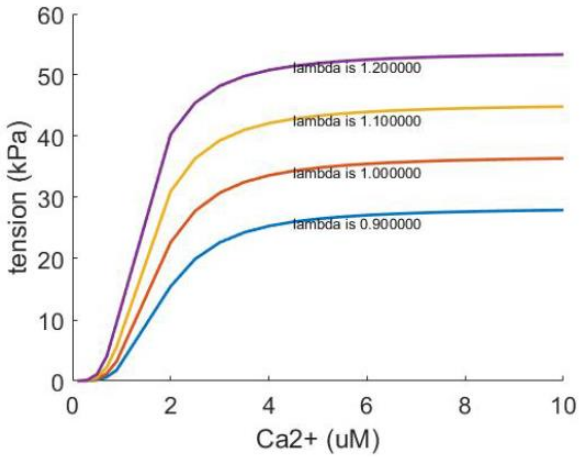

Figure 9: The relationship between the level of Ca2+ and the tension formed in the cardiac muscles during active contraction at different sarcomere lengths.

8. Further Parameter Sensitivity Study

Tables 1 illustrates the data used for studying sensitivity of diff t parameters in the myocyte model.

Table 1: Selected parameters for a Intact Myocyte

TRPN 50	$[Ca^{2+}]_{T50}$	β_0	β_1	Tref	Relative change
.18	0.40	1.15	-1.2	60.25	-50 %
.26	0.60	1.73	-1.8	90	-25 %
.35	0.81	2.30	-2.4	120	0 %
.44	1.01	2.88	-3.0	150	25 %
.53	1.21	3.45	-3.6	180	50 %
.70	1.61	4.60	- 4.8	240	100 %

β0 Parameters

Table 1: Effects of β0 on peak active tension with stretch ratio 1.0.

Intact Myocyte		
β_0	Peak active tension (kPa)	Relative change
1.15	50	0 %
1.73	50	0 %
2.30	50	0 %
2.88	50	0 %
3.45	50	0 %
4.60	50	0 %

The β0 is a length-dependent parameter which represents the change in maximal tension, based on the changes in fi ent overlap. The isometric active contraction with fi stretch ratio 1.0 is studied in intact myocyte cells, with reference to variation of the β0 parameters and its respective effect on the tension developed in the muscle. For β0, in fi 4.10, the left side being active tension from β0 = minvalue, which is 1.15, and the right side being β0 = maxvalue, which is 4.6. With increased β0, the peak active values of tension developed in the muscle remains constant. Based on these results, for intact myocyte cells, the value of the maximum tension attained remains constant at all levels of β0 parameter (i.e., it does not affect peak tension since in the simulation the length is fi for isotonic tension experiments).

β1 Parameters

The β1 is a length-dependent parameter, which captures the change in calcium sensitivity. The isometric active contraction, with fi stretch ratio 1.0, is studied in intact myocyte cells, with reference to the variation of the β1 parameters and its respective effect on the tension developed in the muscle. For β1, in fi 4.11, the left side being active tension from β1 = minvalue, which is -1.2, and the right side being β0 = maxvalue, which is -4.8. With increased β1, the peak active values of tension developed in the muscle remains constant. Based on these results, for intact myocyte cells, the value of the maximum tension attained remains constant at all levels of the β1 parameter (i.e., it does not affect peak tension since in the simulation the length is fi for isotonic tension experiments).

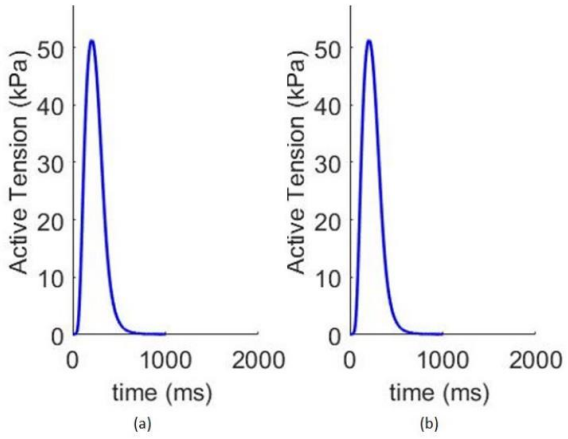

Figure 10: Effects of β0 on active tension development with stretch ratio 1.0, (a) β0 = 1.15; (b) β0 = 4.6. The prescribed calcium profi are same for all simulations, as shown in fi 4.6(a).

Table 2: Effects of β1 on peak active tension with stretch ratio 1.0

Intact Myocyte		
β_1	Peak active tension (kPa)	Relative change
-1.2	50	0 %
-1.8	50	0 %
-2.4	50	0 %
-3.0	50	0 %
-3.6	50	0 %
-4.8	50	0 %

[Ca²⁺]T50 Parameter

We studied the isometric behavior of the [Ca2+]T50 and how it influences the amount of tension generated in cardiac muscles. The effects of [Ca2+]T50 on the tension developed in the muscle depends on the amount of stretch ratio 1.0. The tension developed in

the muscle increased initially with an decrease of the [Ca2+]T50 parameter profile The isometric effects of the [Ca2+]T50 on the tension developed in the cardiac muscle is presented in fi 4.12(a) and 4.12(b). On the right side is the active tension developed at [Ca2+]T50=0.40 on a stretch ratio of 1.0. The maximum tension achieved at this [Ca2+]T50 level is 115kPa. The sub-figure on the right represents the tension developed in the in- tact myocyte at 1.61 µM of [Ca2+]T50. The maximum tension developed at this calcium [Ca2+]T50 is 0.9kPa on a stretch ratio of 1.0. Based on these results, for an intact myocyte cells, the value of the peak active tension decreases with increased [Ca2+]T50 parameter on a stretch ratio of 1.0.

Table 3: Effects of [Ca2+]T50 on peak active tension with stretch ratio 1.0

Intact Myocyte		
$[Ca^{2+}]_{T50}$	Peak active tension (kPa)	Relative change
0.40	115	113 %
0.60	95	90 %
0.81	50	0 %
1.01	16	-68 %
1.21	4.4	-91.2 %
1.61	0.9	-0.98.2 %

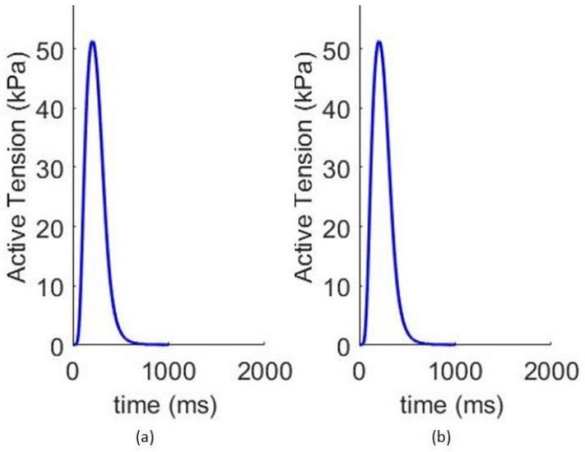

Figure 11: Effects of β1 on active tension development with a stretch ratio 1.0, (a) β1 = −1.2; (b) β1 = −4.8. The prescribed calcium profile are the same for all simulations, as shown in Fig. 6(a).

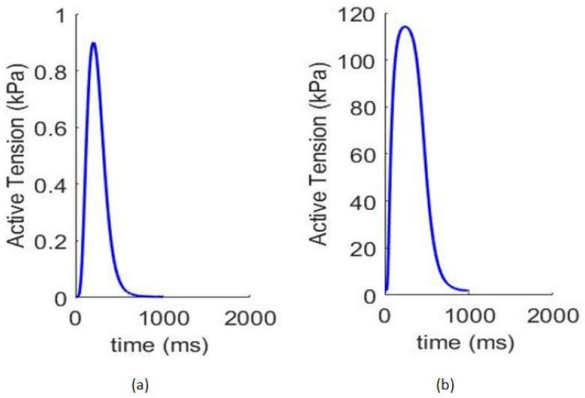

Figure 12: Effects of [Ca2+]T50 on active tension development with stretch ratio 1.0, (a) [Ca2+]T50 = 0.40; (b) [Ca2+]T50 = 1.61. The prescribed calcium profi are the same for all simulations, as shown in fi 4.6(a).

Table 4: Effects of Tref on peak active tension with stretch ratio 1.0

Intact Myocyte		
Tref	Peak active tension (kPa)	Relative change
60.25	25	-50%
90	39	-22 %
120	50	0 %
150	61	22 %
180	79	58 %
240	100.5	101 %

Tref Parameter

We examined the isometric effects of the Tref parameter on the tension developed in the intact myocyte cells. Figure 4.13 contains two subfigures that illustrate the effects of the Tref parameter on the tension developed in the muscle. We observe that the maximum active tension achieved is 60.25kPa for the intact myocyte at Tref=25, based on the sub-figure on the left side. On the other hand, the sub-figure on the right shows that the peak active tension is 100.5 kPa when the Tref is 240kPa. The peak active tension increases with increased Tref parameter in the intact myocyte. Based on these results, the peak active tension increases with an increased Tref parameter in the intact myocyte with stretch ratio of 1.0.

TRPN50 Parameter

Table 5: Effects of TRPN50 on peak active tension with stretch ratio 1.0

Intact Myocyte		
TRPN50	Peak active tension (kPa)	Relative change
0.18	112	124%
0.26	90	80 %
0.35	50	0 %
0.44	24	-52 %
0.53	10.2	-79.6 %
0.70	2.8	94.4 %

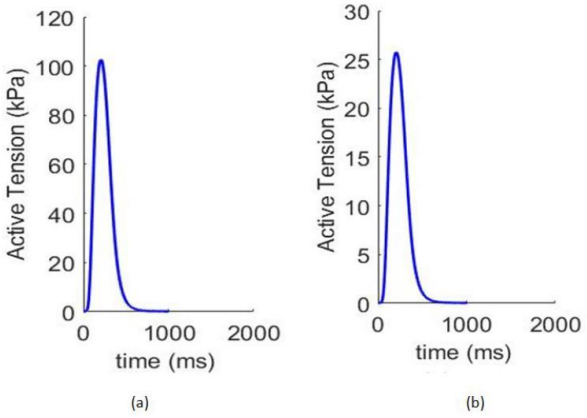

Figure 13: Effects of Tref on active tension development with stretch ratio 1.0, (a) Tref = 60.25; (b) Tref = 240.

The prescribed calcium profile is same for all simulations, as shown in Fig. 6(a).

We studied the effects of the TRPN50 parameter on the tension developed in the cardiac muscle, examining the parametric behavior of the tension by varying the TRPN50 parameter at stretch ratio 1.0. According to sub-figures 4.14(a) and 4.14(b), the tension developed in the muscle increased initially with a decrease in the TRPN50 parameter profi Based on these results, for intact myocyte cells, the value of the peak active tension decreases with increased TRPN50 parameter on a stretch ratio of 1.0.

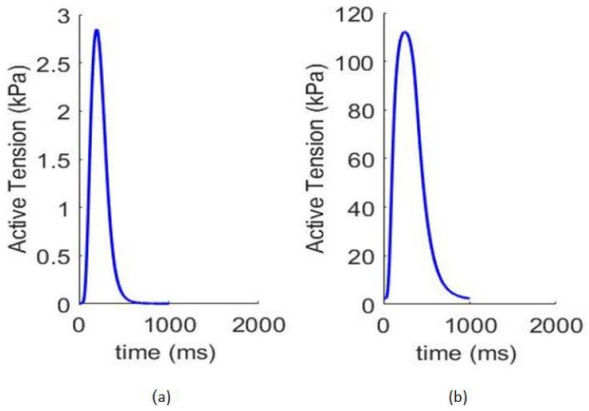

Figure 14: Effects of TRPN50 on active tension development with stretch ratio 1.0, (a) TRPN 50 = 0.18; (b) TRPN 50 = 0.7. The prescribed calcium profile is the same for all simulations, as shown in Fig. 6(a).

9. Functionality and Limitations of the Model

The Land model used in this study is able to closely reproduce the saturating value of the force (tension) for corresponding sarcomere lengths. However, there are some differences between simulated and experimental data in sensitivity to an external Ca2+, as simulated force saturates at lower values of Ca2+ concentrations. Such diff are due to a decrease in Ca2+ sensitivity of skinned compared to intact cardiac cells. In addition, the current model can reproduce a shift in Ca2+ sensitivity for steady-state force-calcium relationships shown for diff t sarcomere lengths (see fi 4.9). Such a shift is seen in normalized steady-state force-calcium relationships. Simulations show that an increase in sarcomere length leads to smaller half-saturation values of Ca2+ concentrations, demonstrating an increase in Ca2+ sensitivity (see Fig. 6). A similar shift in Ca2+ sensitivity was also observed experimentally for mouse cardiac cells.

The model of cardiac myocyte contraction also has some limitations due to the simplify of the biophysical mechanism of contraction. Specifically, the model uses a simplified description of the relationships between contraction force and cellular shortening in the form of Hooks law, while the real dependence is more complicated. It does not describe the effects of cellular shortening on Ca2+ transients, as does the Land model. However, this effect is relatively small. Also this model, as with most other models, did not take into account intracellular spatial in-homogeneities of Ca2+ concentration and cross-bridges binding sites.

3 Conclusion

This project focused on studying mathematical models of the cardiac myocyte's active contraction. Various models have been developed based on existing studies and various concepts about the functionality of the cardiac muscle in humans [10]. The functionality of the heart is enabled by the cardiac muscles that contract to promote the ow of blood to deferent parts of the body.

In this work, we worked on mathematical modelling of myocyte by using the Land model, which was developed based on real experimentation. The mathematical models simulated in this project were based on the existing models in the Land model.

The limitations of the Land model use include: 1) a simplified description of the relationships between the contraction force and the cellular shortening in the form of Hooks law, while the real dependence is more complicated. 2) a lack of description of the effects of cellular shortening on Ca2+ transients, as with the Land model, although this effect is relatively small. Last but not the least, this model, like most others, does not take into account intracellular spatial in-homogeneities of Ca2+ concentration and crossbridge binding sites.

The main objective was then directed to the study of the Land model, which we used to simulate the contraction of real human myocytes. By using this model, we successfully simulated myocyte contraction for deferent scenarios, such as in isometric tension and isotonic tension. We found that with increased stretch, the peak active tension increases, in line with well-established length-dependent tension generation. Five parameters were selected: [Ca2+]T50, Tref, TRPN50, _0 and _1. Each parameter was varied between -50% to 100%, in order to examine the isometric effects of each parameter on the behavior of the tension developed in the intact myocyte cells, with the most sensitive parameter being [Ca2+]T50. In conclusion, it was found that the Land model provides a good platform for the analysis of the active contraction of the human cardiac myocyte.

References

[1] S. Land et al. A model of cardiac contraction based on novel measurements of tension development in human cardiomyocytes. Journal of Molecular and Cellular Cardiology, 106:68–83, 2017.

[2] J. Keener and J. Sneyd. Mathematical Physiology I: Cellular Physiology, Second Edition. 2009.

[3] J. Keener and J. Sneyd. Mathematical Physiology II: Systems Physiology, Second Edition. 2009.

[4] F. Asiri, Modeling of Human Myocyte Active Contraction: A Review, VW Appl. Sci., vol. 1, no. 1, pp. 26-31, Sep. 2019.

[5] F. Asiri, Mathematical Modeling of General

Muscle Contraction, VW Engg. Int., vol. 1, no. 1, pp. 27-34, Oct. 2019.

[6] R. Ruiz-Baier et al. Mathematical modelling of active contraction in isolated cardiomyocytes. Mathematical Medicine and Biology, 31.3:259–283, 2014.

[7] M. D. Stern. Theory of excitation-contraction coupling in cardiac muscle. Biophysical journal, 63.2:497–517, 1992.

[8] S. Vasileiou. Feedback between mechanical contraction and electrical excitation in cardiac cells. University Of Glasgow, 2016.

[9] D. M. Bers. Cardiac excitation-contraction coupling. Nature, 415.6868:198–205, 2002.

[10] E. M. Cherry and F. H. Fenton. Heart structure, function and arrhythmias. The Virtual Heart, Department of Biomedical Sciences, College of Veterinary Medicine, Cornell University.

[11] D. M. Bers. Excitation-contraction coupling and cardiac contractile force., volume 237. 2001.

[12] D. G. Allen and J. C. Kentish. The cellular basis of the length-tension relation in cardiac muscle. Journal of molecular and cellular cardiology, 17.9:821–840, 1985.

[13] P. J. Hunter, A. D. McCulloch, and H. E. D. J. Ter Keurs. Modelling the mechanical properties of cardiac muscle. Progress in biophysics and molecular biology, 69.2:289– 331, 1998.

[14] S. Vasileiou. Feedback between mechanical contraction and electrical excitation in cardiac cells. University Of Glasgow, 2016.

[15] N. Burns. Cardiovascular physiology. Physiology, School of Medicine, Trinity Col- lege, Dublin, 2013.

[16] T. Jarm, P. Kramar, and A. Zupanic. 11th Mediterranean Conference on Medical and Biological Engineering and Computing 2007: MEDICON 2007, 26-30 June 2007, Ljubljana, Slovenia., 16, 2007.

[17] V. Hill. The heat shortening and the dynamic of constants of muscle. Proc. R. Soc. Lond. B, 126:136–195, 1938.